3-D Printed Customizable Vitrification Devices for Preservation of Genetic Resources of Aquatic Species

Journal: *Aquacultural Engineering*

Connor J. Tiersch[a1], Yue Liu[b], Terrence R. Tiersch[c], William T. Monroe[b, *]

[a] Craft & Hawkins Department of Petroleum Engineering, Louisiana State University, 3207 Patrick F. Taylor Hall, Baton Rouge, Louisiana 70803, USA

[b] Department of Biological & Agricultural Engineering, Louisiana State University, 149 E. B. Doran Building, Baton Rouge, Louisiana, 70803, USA

[c] Aquatic Germplasm and Genetic Resources Center, School of Renewable Natural Resources, Louisiana State University Agricultural Center, 2288 Gourrier Avenue, Baton Rouge, Louisiana, 70820, USA

[1] Present address: Aquaculture Systems Technologies, LLC, 2120 N. 3rd Street, Baton Rouge, Louisiana, 70802, USA

Corresponding author:
W. Todd Monroe, PhD
163 E. B. Doran Building, Department of Biological and Agricultural Engineering, Louisiana State University, Baton Rouge, LA 70803, USA
Email: tmonroe@lsu.edu

Abstract

Sperm vitrification as an alternative approach to conventional cryopreservation (equilibrium freezing) allows quick and low-cost sample preservation and is suitable for small-bodied aquatic species with miniscule testis, fieldwork at remote locations, and small-scale freezing for research purposes. The goal of this present study was to develop operational prototypes of 3-dimensional (3-D) printed vitrification devices with innovative components that can provide comprehensive functionalities for practical repository development for aquatic species. The design featured an elongated loop to suspend a thin film of sperm sample in cryoprotectant, a retractable sleeve to protect the vitrified samples and allow permanent labeling, a handle to facilitate processing and storage, and a shaft with annular grooves to guide positioning of the protective retractable sleeve. To span a wide range of sample capacities and configurations, a total of 39 different configurations (3 loop lengths ×13 loop heights) were fabricated by 3-D printing with the thermoplastics polylactic acid (PLA) and acrylonitrile butadiene styrene (ABS). A total of 86 devices were fabricated with ABS filament with a print failure rate of 9%, and 97 devices were fabricated with PLA filament with a failure rate of 20%. Major types of printing failures included disconnected loops, insufficient build surface adhesion, stringing, and inconsistent extrusion. The sample volume capacity ranged from 1-47 μL and had linear relationships to the loop lengths and layer numbers. Vitrified samples were observed in 10-mm and 15-mm loops fabricated with PLA and ABS but not in 20-mm loops. This study demonstrated the feasibility of development of standardized low-cost ($0.05 material cost) devices fabricated by 3-D printing with practical functions including vitrification, volume control, labeling, protection, and storage within conventional systems. These prototypes can be further developed, standardized, and used to assist development of germplasm repositories to protect the genetic resources of aquatic species by user groups such as breeders, hatcheries, aquariums, and researchers.

Keywords: 3-D printing, sperm vitrification, device, low-cost, standardization, aquatic species

Introduction

Development of germplasm repositories to protect the genetic resources of aquatic species has been hindered by several factors over the past 70 years including an almost complete focus on cryopreservation research and protocol development. Other problems include a lack of approaches for standardization, and the requirement to adapt equipment and supplies developed for livestock and human medicine for use with fish and shellfish. New fabrication technologies such as 3-dimensional (3-D) printing can provide expanded access to CAD-CAM capabilities, and open new opportunities for custom design and production of standardizable devices directly based on the needs of aquatic user communities. Inexpensive devices such as these can be distributed as open-source files to facilitate application, and to support and focus protocol development, ensuring that high-quality material can be made available to centralized germplasm repositories.

Because of the current lack of repository development, the utility of cryopreservation remains largely unrealized for aquatic species in multiple areas including genetic improvement for aquaculture (Blackburn, 2011; Hu et al., 2011), stock enhancement for wild fisheries (Riley et al., 2004; Tiersch et al., 2004), protection of genetic diversity in imperiled species (Liu et al., 2018; Wayman et al., 2008), and storage and distribution of tens of thousands of research lines of biomedical research models (Torres et al., 2017; Yang and Tiersch, 2009). Cryopreserved sperm has been incorporated into germplasm repositories for protection and management of genetic resources in other species such as livestock (Purdy et al., 2016), but that is because they have moved past protocol research into application, often by utilization of engineering approaches.

Efforts in application of engineering technologies for sperm cryopreservation have primarily focused on conventional cryopreservation (‘equilibrium freezing’) methods. A critical factor

81 determining the success of equilibrium freezing is to identify and achieve ideal cooling rates (e.g.,
82 5-40 °C/min) during freezing (Hezavehei et al., 2018). Control of cooling rate requires
83 specialized equipment, which can cost tens of thousands of dollars for computer-programmed
84 types or several thousand dollars for other types.
85
86 An alternative and relatively new method for sperm cryopreservation is vitrification, by which
87 liquid is cooled at > 1,000 °C/min ('rapid cooling') to transform into an amorphous solid (glass)
88 phase without the formation of crystalline ice (Cuevas-Uribe et al., 2017; Rall and Fahy, 1985).
89 The rapid cooling can be obtained simply by plunging a thin film (e.g., several µl loaded on
90 loops) or droplets (e.g., on plates or strips) of sample into liquid nitrogen. As such, vitrification
91 allows low-cost sample preservation (Magnotti et al., 2018) and is suitable for: (1) small-bodied
92 species with miniscule sample volumes, (2) fieldwork at remote locations where equipment or
93 electricity are not accessible, and (3) small-scale freezing for research purposes. For example,
94 swordtails and guppies (family Poeciliidae) are popular ornamental and aquaculture species in the
95 U.S. and typically provide < 5 µl of sperm from each male (Huang et al., 2009; Yang et al.,
96 2009), and thus vitrification could be an ideal method for preserving sperm of these species for
97 genetic management purposes (Cuevas-Uribe et al., 2011b).
98
99 There are several major limitations of existing devices (i.e., with specialized vitrification
100 functions) and tools (i.e., designed for applications other than vitrification) used in sperm
101 vitrification. Firstly, most commercial vitrification devices previously reported were designed for
102 freezing of mammalian oocytes and embryos, and thus only accommodate small sample volumes
103 (e.g. < 2 µl) for sperm loading. For example, the Cryotop® devices (KITAZATO, Valencia,
104 Spain), designed for vitrification of human oocytes and embryos, were used in sperm vitrification
105 of Eurasian perch (*Perca fluviatilis*) and European eel (*Anguilla anguilla*) (Kása et al., 2017).
106 However, only 2 µl of sperm suspension could be loaded onto each device (Marco-Jiménez et al.,

2016). Secondly, devices specifically designed for sperm vitrification are often medical devices intended for human clinical application, and thus these devices are costly. For example, the Cryotop® costs more than $20/device. The Sperm VD device (Berkovitz et al., 2018) designed for sperm vitrification with storing and labeling mechanisms costs $60 and can only load about 1 µl of sample per device. Thirdly, non-specialized tools have been adopted for sperm vitrification. For example, a study of sperm vitrification of channel catfish (*Ictalurus punctatus*) evaluated various options (Cuevas-Uribe et al., 2011a), such as pipette tips (originally for liquid transfer), sperm cryopreservation straws (for equilibrium freezing of semen) cut at various angles, and inoculation loops (for microbiology). Although these tools can help reduce costs and some of them can provide limited functionality for operation and sample recovery, they lack the capability to be customized, standardized, securely labeled, and efficiently stored.

Recently, the increasing availability of consumer-level 3-D printing makes it possible to rapidly prototype and fabricate devices at a low cost. This technology has been introduced to the field of cryobiology (Hu et al., 2017; Tiersch and Monroe, 2016) and repository development for aquatic species (Tiersch and Tiersch, 2017). Previous work has demonstrated the feasibility of using 3-D printed loops with a material cost of $0.01/unit to perform sample vitrification (Tiersch et al., 2019). Given the feasibility of vitrification within 3-D printed loops (a single component) the next step is design and test operational devices (multiple integrated components), with additional features to achieve practical capabilities and functionalities, such as handling, sorting, labeling, and storage. The goal of the present study was to develop and test operational prototypes of low-cost 3-D printed sperm vitrification devices with innovative elements that can provide comprehensive functionalities for practical repository development for aquatic species. The specific objectives were to: (1) design component prototypes and operational prototypes; (2) evaluate fabrication feasibility with consumer-grade 3-D printers; (3) evaluate the relationship of sample volume capacity with various configurations, and (4) evaluate the feasibility of

operational prototypes to achieve vitrification. The innovation of these operational prototypes can provide a foundation for further performance testing, and divergent modifications, and ultimately standardization (as a long-term goal) based on the needs of user communities.

Methods

Design of prototypes

Computer-aided design (CAD) software (Inventor® Autodesk, San Rafael, CA) was used to create 3-D designs of prototypes. Based on concepts of previous studies (Tiersch et al., 2019; Tiersch and Tiersch, 2017), the present study (Fig. 1A) integrated several innovative components and functions, including: (1) a loop to suspend a thin film of fluid (i.e. sperm suspension); (2) a retractable sleeve to protect vitrified samples and allow permanent labeling by ink-jet printing; (3) a handle to facilitate processing and storage; (4) a shaft with annular grooves to position the protective retractable sleeve in the "open" (freezing position) or "closed" (storage position) positions, and (5) a detent inside the retractable sleeve to fit the annular grooves for appropriate positioning. For prototyping, identification jackets from commercially available 0.5-mL sperm cryopreservation straws (Cryo Bio System, L'Aigle, France) (referred to as 'CBS straws') were used as protective retractable sleeves These jackets can be labeled by automated straw printers such as MAPI (CBS) and Quattro (Minitube, Tiefenbach, Germany) systems, and have been evaluated for use with aquatic species (Hu et al., 2011).

The design constraints included: (1) the width and thickness (Fig. 2) of the loop must be less than the inner diameter (ID) of the protective retractable sleeve (ID = 3.1 mm); (2) the length of the shaft must be greater than the length of the protective retractable sleeve (50.0 mm); the overall length of the device must be less than the length of common cryopreservation straws (~134 mm);

(4) the minimum feature thickness must be ≥ 0.2 mm due to current limitations of the 3-D printers used; (5) the geometry of 3-D models should be suitable for fabrication by fused-deposition modeling (FDM) 3-D printers (e.g., no overhang structures), (6) and the material cost of each device should be < $0.05. Dimension variations in the loop length and loop thickness were created to characterize sample volumes and performance in vitrification testing.

Evaluation of fabrication feasibility

The 3-D models of prototypes were converted to stereolithography (STL) files in the Inventor software and imported into a slicing software (MakerBot Desktop Beta, MakerBot, New York City, New York). The default "standard" settings in the software were used for fabrication (Table 1). The printing settings and 3-D models were converted to G-Code format (transferred by a SD card) and imported to an FDM-type 3-D printer (MakerBot Replicator 2X, MakerBot).

Different versions of prototypes were initially designed to evaluate the functionality of individual components, and suitable versions of each component were chosen to evaluate the operation of integrated prototypes (operational prototypes). In operational prototyping, a total of 39 dimensional configurations (3 different loop lengths × 13 different layer numbers) were printed with filament (1.75 mm diameter, MakerBot) of two thermoplastic materials: polylactic acid (PLA) and acrylonitrile butadiene styrene (ABS). The PLA filament was printed at 200 °C (heat block temperature) on an unheated (room temperature) print bed. The ABS filament was printed at 230 °C (heat block temperature) on a heated (110 °C) print bed. The printing environment (room 116 at the Aquatic Germplasm and Genetic Resources Center) was controlled at 24-26 °C (adjusted by a central air conditioner) and a humidity of 46-53% (adjusted by a dehumidifier).

It took ~ 5 min (not including heating) to print each device. After each batch of printing, the fabricated prototypes were visually inspected. Undesired deformities were recorded and categorized as fabrication failure. The prototypes with fabrication print failures were reprinted until a total of 156 failure-free devices (3 loop lengths ×13 loop heights × 2 thermoplastics × 2 duplicates) were printed for evaluation. The print failure rate was calculated as: (the number of fabrication failures)/(the total number fabricated). The layer height of each layer number was measured with a digital caliper (Neiko 01407A). The increment layer height was calculated as the height differences between two contiguous layer numbers. The layer height of layer number 1 equaled to the first increment layer height. A total of 13 increment layer heights were averaged for 13 layer numbers.

Evaluation of sample volume capacity

Deionized water was used to initially evaluate the sample volume capacity of various configurations to provide a standardizable testing method (Tiersch et al., 2019). Water has broad accessibility and standard physical properties, enabling researchers around the world to compare results. In addition, the mass of water can be easily and precisely converted to volume at known temperature. In contrast, typical cryoprotectant and extender solutions used for vitrification are widely divergent in physical and chemical properties, and are typically admixtures with multiple components that make it extremely difficult to precisely calculate volume based on mass measurement. Finally, films formed with water are often less stable than those formed by high-viscosity vitrification solutions, and can provide a conservative measure for evaluation of film failure. The loop section of each prototype was submerged into deionized water to form a film. An analytical balance (Mettler, AE 166, Columbus, OH) was used to measure the mass (mg) of the devices before and after film formation. The recorded masses were converted into volumes in

209 μL using the relationship between mass and volume of deionized water (1:1 at 4 °C, corrected for
210 testing at 24 °C).
211
212 *Evaluation of vitrification feasibility*
213
214 Vitrification occurrence was evaluated with a vitrification solution (20% Hanks' balanced salt
215 solution, 40% methanol, methyl glycol 20%, 1,2 propanediol 20%) described in previous studies
216 (Cuevas-Uribe et al., 2011a; Tiersch et al., 2019). All solutions were stored at 4 °C between
217 testings, and were mixed thoroughly before each use. Prior to sample loading, the protective
218 retractable sleeve was slid to the "open" position (Fig. 2). A loop was submerged into the
219 vitrification solution to form a film, followed by plunging of the loop into liquid nitrogen
220 (Cuevas‐Uribe et al., 2015). The loop remained submerged in the liquid nitrogen while the
221 retractable sleeve was slid to the "closed" position (Fig. 3). Prototypes with frozen films were
222 transferred into a daisy goblet within liquid nitrogen, and subsequently transferred into a liquid
223 nitrogen dewar for storage for at least 24 hr.
224
225 To determine vitrification quality, a standardized evaluation method (Tiersch and Tiersch, 2017)
226 previously established was used. Briefly, after removal from liquid nitrogen, the frozen films in
227 loops were precisely positioned in front of a viewing panel on a custom 3-D printed pedestal, and
228 visually examined. Vitrification quality was classified by clarity of the frozen film as determined
229 by the visibility of parallel horizontal lines on the viewing panel. Frozen films were classified as:
230 (1) 'Film failure' (indicating there was a fracture or absence of the film within the loop), (2)
231 'Opaque' (film was intact with low clarity, indicating abundant crystalline ice formation), (3)
232 'Translucent' (film was intact with high clarity but not full transparency, indicating partial
233 vitrification), or (4) 'Transparent' (film was intact with full transparency, indicating substantial

vitrification or glass transition). To perform the determination of vitrification quality in a standardized manner (Tiersch et al., 2019; Tiersch and Tiersch, 2017), two people (assessor and recorder) were used to conduct experimentation. Assessments were made as the recorder started a timer when the assessor said "start," which signified the removal of a vitrification device from liquid nitrogen. The assessor placed the device on the pedestal (aligning the film in front of the viewing lines) and voiced a classification. The recorder immediately stopped the timer and documented the time of assessment and the classification. The time between when the assessor removed a device from liquid nitrogen until voicing the classification was the documented time of assessment. Samples were assessed in a walk-in refrigerated room, which remained at 4-7°C with 65-70% relative humidity. A maximum time for assessment was set at ≤ 2.5 sec to ensure that classifications were assigned before the films began to thaw.

Statistical analysis

All statistical analyses were performed using SAS 9.4 (SAS Institute, NC, USA). A one-sample *t*-test (PROC TTEST) was used to compare the difference between the nominal (0.2 MM) and measure increment layer height. A paired *t*-test (PROC TTEST 'PAIRED') was used to compare the sample volume capacity of prototypes fabricated with ABS and PLA. Simple linear regression analyses (PROC REG) were performed to evaluate the relationship between the sample volume capacity and the layer number of loops. The vitrification quality of 'Film failure' < 'Opaque' < 'Translucent' < 'Transparent' classifications were considered as ordinal data. A Wilcoxon-Mann-Whitney test (PROC NPAR1WAY) was used to compare the vitrification quality between devices fabrication by ABS and PLA, and a Friedman's test (PROC FREQ) with repeated measures was used to compare vitrification quality among devices with different loop lengths. Logistic regression (PROC LOGISTIC) analyses were used to analyze the relationship between vitrification quality and loop layer numbers. For the logistic regression, the vitrification quality

values were converted to binary data as ‘vitrified’ and ‘not vitrified’, and the loop length of 20 mm was eliminated (because no vitrification was formed in this group) to satisfy assumptions for the analyses. The results were considered statistically significant at $P < 0.05$.

Results

Design of prototypes

Based on 32 versions of initial component prototypes (data not shown), the design of operational prototypes was developed (Fig. 2) and evaluated. The loop featured a lanceolate shape with configurations of three different lengths (10, 15, and 20 mm) and 13 different thicknesses. Thirteen layers was the maximum that could fit within the protective retractable sleeve (0.2 to 2.6 mm based on 1 to 13 layers of thermoplastic deposition with a nominal 0.2-mm thickness of each layer). The handle length was designed to be 49 mm to be sufficiently long to avoid cryogenic injury to users when submerging the loop in liquid nitrogen. An overall length of 127 mm ensured that the device could fit into commercially available Daisy goblets (about 135 mm in height when covered by lids) (IMV Technologies, L'Aigle, France), which are commonly used for sorting and storage of sperm cryopreservation straws (about 133 mm in length). Annular grooves with widths of 2 and 4 mm were designed on a shaft to enable the sliding and positioning of a CBS retractable sleeve for sample protection and identification.

Evaluation of fabrication feasibility

A total of 97 operational prototypes were fabricated with PLA filament with a print failure rate of 20% (Fig. 4A), and 86 prototypes were fabricated with ABS filament with a print failure rate of 9%. Four major types of printing failures (Fig. 5) were observed, including: (1) disconnected

loops (non-continuous deposition and gaps on loops), (2) poor build surface adhesion (e.g., a portion of the loop was warped inwards), (3) stringing (thin strands of plastic caught on the loop), and (4) inconsistent extrusion (droplets of extra plastic deposited periodically along the print path), due to inconsistent feeding rate of filament.

The actual measurement of layer height increment was 0.19 mm to 0.20 mm. No significant differences ($0.1545 < P < 0.8920$) in layer height increment were found between the actual measurement and nominal increment (0.2 mm) (Fig 4B).

Evaluation of sample capacity

The sample volume capacity ranged from 1-26 μL for prototypes with 10-mm loops, 1-32 μL for 15-mm loops, and 1-47 μL for 20-mm loops (Fig. 6). The sample capacity of prototypes fabricated with PLA was significantly ($P < 0.0001$) higher than those fabricated with ABS in all three loop lengths. In all materials and loop lengths, the sample volume capacity had a significant ($P < 0.0001$, $r^2 > 0.98$) relationship with the layer number (i.e., the volume increased with layer number), and loop length ($P < 0.0001$, $r^2 = 0.93$) (i.e., volume increased with loop length).

Evaluation of vitrification feasibility

No prototypes were damaged due to exposure to liquid nitrogen. The average assessment time was ~ 14 sec from initial submersion into cryoprotectant solutions for sample loading, through dipping into liquid nitrogen for freezing. For quality evaluation, samples were assessed for vitrification classification within 2.5 s of removal from liquid nitrogen (Tiersch et al. 2019). Vitrified samples (transparent frozen films) were observed in 10-mm and 15-mm loops fabricated with PLA and ABS, but not in 20-mm loops. Among 10-mm and 15-mm configurations,

312 vitrification feasibility was observed in PLA loops with 1-6 layers and ABS loops with 1-3 layers.
313 Film failures were observed in all layer numbers in the 20-mm configurations.
314
315 No significant differences ($P = 0.0679$) were found in vitrification quality between prototypes
316 fabricated using ABS and PLA filaments. Vitrification quality decreased significantly ($P <$
317 0.0001) with loop length. Logistic regression (Fig. 7) indicated that the probability of vitrification
318 decreased significantly ($P = 0.0039$) with increasing number of loop layers. The Hosmer-
319 Lemeshow goodness-of-fit test showed strong prediction ($\chi^2 = 4.2876$, d.f. = 8, $P = 0.8303$) of the
320 logistic model.
321
322 **Discussion**
323
324 Basic methods for cryopreserving gametes of aquatic and livestock species were each first
325 developed about 70 years ago (Blaxter, 1953; Polge and Rowson, 1952), and since then
326 cryopreserved sperm of livestock has grown into a multi-billion-dollar global industry (Hu et al.,
327 2011), but aquatic species remain at initial stages with tremendous growth potential. Some
328 progress has been made, for example, the National Animal Germplasm Program (NAGP) of the
329 U.S. Department of Agriculture, a national repository established for agricultural animals,
330 currently includes more than 7,000 individuals comprising 110,000 samples from freshwater and
331 marine aquatic species (Animal-GRIN, 2019; Blackburn, 2011). However, there is no integrated
332 set of practices available to reliably collect, process, cryopreserve, transport or use aquatic species
333 samples in repositories or in commercial germplasm markets (Torres and Tiersch, 2018). As
334 indicated above, a critical problem that impedes application of cryopreservation in aquatic species
335 is the lack of innovative technologies that can provide inexpensive, standardized, and practical
336 devices for a wide range of users such as breeders hatcheries, aquariums, researchers, and
337 repository operators (Hagedorn et al., 2019).

338

339 *Rapid prototyping of cryopreservation devices with 3-D printing*

340

341 In the past several years, 3-D printing technology has become available and affordable, providing
342 tremendous opportunities for development of innovative technologies for aquaculture research
343 (Hu et al., 2017; Tiersch and Monroe, 2016). With the rapid prototyping capabilities provided by
344 3-D printing (Rayna and Striukova, 2016) and computer-aided design software (Ho et al., 2015),
345 innovative ideas can be fabricated as prototypes to be tested within minutes for small objects,
346 such as the devices evaluated in this study.

347

348 We recognize three major phases in the rapid prototyping process for device development. In the
349 first phase (component prototyping), ideas are transformed into designs, which are subsequently
350 fabricated into prototypes of individual components (e.g., loops only). Functionalities of these
351 components are evaluated individually, design changes are made, and different versions of
352 "component prototypes" are developed. In the second phase (operational prototyping), suitable
353 versions of the component prototypes are integrated into composite devices (e.g., loops plus
354 handles and sleeves). The operation of integrated protypes ("operational prototypes") are
355 evaluated and multiple "variations" are developed. In the third phase (performance prototyping),
356 advanced operational prototypes ("performance prototypes") are tested for performance,
357 including biological utility, reproducibility, reliability and efficiency, and further refinements are
358 made. The goal of the present study was to develop operational prototypes of a 3-D printed
359 vitrification device, which can be further evaluated as performance prototypes. The long-term
360 goal is to develop standardized vitrification devices that can be made available to aquatic user
361 communities.

362

363 *Design of prototypes*

Efficient handling, appropriate storage, and secure labeling of cryopreserved samples are essential in preservation and utilization of germplasm resources (Torres and Tiersch, 2018). The design of operational prototypes featured a loop with variable configurations, a handle, a shaft with annular grooves on it, and a retractable protective sleeve. The function of the loops was to support a thin film of sample to enable a sufficiently high cooling rate to achieve vitrification. The widths of the loops were constrained by the inner diameter of the retractable sleeves, which were adopted from commercially available CBS labeling jackets. To enhance sample volume capacity, the loops were designed as lanceolate shapes instead of circles to maximize loop length. The retractable sleeve was necessary for practical operation during sorting, shipping, and long-term storage, in which there is a risk of samples contacting other objects, resulting in detachment of loops. The annular grooves on the shaft provided standardized positioning of the protective sleeve to ensure full coverage of the loop in the low visibility conditions often encountered when working with liquid nitrogen due to condensation.

In addition to protection, this retractable sleeve could be labeled by commercial-scale straw filling, sealing, and printing equipment, (such as the MAPI (CBS) and Quattro (Minitube), or research-scale tags, such as Cryo-StrawTAG™ (GA International, Quebec, Canada). The handle provided efficiency when gripping the device with two fingers (without reliance on tools such as tweezers) during operations, including freezing, sliding the retractable sleeve, sorting, loading into containers, quality evaluation, and thawing. After freezing and closure of the sleeve, the samples could be sorted and stored within Daisy goblets, which are commonly used for sperm cryopreservation straws, and thus did not require custom container development.

In future studies, other choices of protective retractable sleeves should be considered. For example, commercially available sperm cryopreservation straws (‘French straws’) (IMV) could

be used as protective retractable sleeves to reduce the cost (several cents per straw) compared to the CBS jackets ($0.15 per jacket sold separately). The CBS jackets used in this study were for prototyping purposes only, although they can be printed with alphanumeric labels on automated equipment.

Fabrication of prototypes

A major advantage of prototype fabrication by 3-D printing is that design files can be shared (supplemental data S1) and prototypes can be replicated easily by users who have access to a 3-D printer (Rayna and Striukova, 2016). The limitation is that this method can allow variations in fabrication quality (Fernandez-Vicente et al., 2016). Even with an identical design, slight variations in parameter settings can result in variable fabrication quality. As such, for different users to replicate prototypes with their own 3-D printers, it is important for the printing parameters to be reported in detail in a standardized way. Undesired fabrication features were observed in the prototypes printed in the present study. However, the fabrication quality can be improved by identifying the causes, adjusting parameters in the slicing software, and re-calibrating the 3-D printers (Devicharan and Garg, 2019; Frauenfelder, 2013).

For example, stringing could be caused by inappropriate settings for retraction (i.e., pulling back a small amount of filament before the nozzle travels between two printing locations), printing temperature (within heat block to melt filament), or printing speed (speed of nozzle travel during deposition of melted plastic). To reduce the stringing defects, settings in the slicing software can be adjusted to increase retraction distance or speed, lower the printing temperature, or lower the printing speed. In addition, the defects of poor build surface adhesion could be addressed by reducing the fan speed of the first layer (used to rapidly cool thermoplastic after extrusion) or by increasing the temperature of the build surface (unheated for PLA in this study). Disconnected

loops could be addressed by careful calibration of build surface leveling, and inconsistent extrusion could be addressed by unclogging the printing nozzle or untangling of the filament as it leaves the spool. We attempted to print the operational prototypes using standard settings as much as possible to allow identification of the problems and defects that would be encountered in general practice. For performance testing and beyond, optimized printer settings could be used.

The measured layer height increment showed no difference with the nominal increment of 0.2 mm for each layer, suggesting that FDM 3-D printing was able to fabricate vitrification loops with specific height reliably. However, the reliability in such small dimension (< 0.5 mm) is highly sensitive to operational settings of 3-D printers and slicing software. Standardized operation of 3-D printing in biological research application should be addressed in future studies.

Evaluation of sample volume capacity

Sample volume capacity is critical for vitrification quality and efficiency (Fahy and Wowk, 2015). Relatively higher volumes can reduce the possibility of vitrification because of inadequate cooling rates, whereas lower volumes can increase the operation cost, time, and storage space requirements (Cuevas-Uribe et al., 2017). Commercially available vitrification devices and tools used for sperm cryopreservation have fixed volumes and are not customizable. Based on the relationships revealed in the present study, sample volume capacity could be controlled by adjusting the length and the height of the loop, providing a customization capability for future development. With these highly correlated relationships, the number of vitrification devices to be used in a freezing operation can be calculated. In this study, water was used as a model to evaluate sample volume capacity to facilitate standard comparisons across studies (actual volumes of sperm cryopreservation solutions may be different based on physical properties). Future designs could include modifications such as multiple loops on a single device to increase

sample capacity. Tailored 3-D printing filaments with widely varying hydrophobicity are becoming more readily available (Jafari et al., 2019), and could be incorporated to optimize film formation and stability in these devices.

The volume of semen collected from small-sized aquatic species, such as swordtails (*Xiphophorus Spp.*), is usually < 10 µL/male without dilution, and about 250 µL after dilution for cryopreservation (e.g., 1×10^8 cells/mL) (Cuevas-Uribe et al., 2011b). The prototypes in this study provided a sample capacity range of 1-10 µL for a single device for about $0.04 (material cost), indicating that the efficiency of these prototypes was superior to commercial sperm vitrification devices (1 µl per device for about $50) (Berkovitz et al., 2018) and can potentially freeze samples from a single male swordtails within 10 devices. Currently, a consumer-level 3-D printer with reliable printing quality costs < $250 (e.g., Creality Ender 3, Shenzhen Creality 3D Technology Co., LTD.), and thus investing in a 3-D printer and printing five devices would be less than the investment for purchasing six commercial vitrification devices, useful only for a single fish ($300).

Evaluation of vitrification feasibility

This study demonstrated the feasibility of vitrifying samples with 3-D printed devices that can fit into labeled retractable sleeves during storage. A previous study (Tiersch et al., 2019) of component prototypes (loops only) investigated loop lengths of 15, 19, and 23.5 mm and 1-6 layers, suggesting that shorter loop lengths and heights could increase vitrification probability. Based on this result, the present study evaluated loop lengths of < 15 mm and increased layer numbers (1-13). The results showed the trend of vitrification probability decreasing with increases in loop length and height were compatible with the previous study. Because the present study was a feasibility evaluation of operational prototype devices, only two replicates for each

prototype configuration were evaluated. The results indicate further investigations can be focused on shorter loop lengths (< 15 mm) and heights (<1.2 mm), based on the occurrence of vitrification in the conditions that were studied. The reduction in vitrification probability might be caused by insulative effects of the thermoplastic (which diminish the ability to transfer heat effectively), and increased sample mass (which could reduce the cooling rate. Further investigation could use simulation modeling techniques to predict vitrification probability by examining the relationship between cooling rate and design geometry (and dimensions). Reproducibility of selected operational prototypes should be characterized in further performance prototyping studies with larger sample sizes (i.e. > 10 duplicates per dimension) to yield more strict statistical comparisons.

Conclusions

This study demonstrated the feasibility of custom fabricating 3-D printed, inexpensive (< $0.1 material cost), and customizable devices with practical functions including vitrification, volume control, labeling, protection, and storage. Overall, it should be recognized that research itself cannot directly lead to standardization. An innovative device (or approach) will not immediately (or naturally) become a standardized device (or approach) without interaction with user communities. After a new method is developed and published, it usually diverges into modifications by individuals within a research community based on different motivations, such as customization, optimization, specification, curiosity, or errors (Liu et al., 2019). Eventually, the modified methods may be integrated and converged into a standardized approach at the community level to enable direct comparison of research results and to foster technology application. The use of 3-D printing in prototyping of innovative devices can greatly facilitate this community-level standardization process. The innovative prototypes in the present study would allow users to make modifications easily with the long-term goal of converging such

494 modifications to yield a generalized community standard. The prototypes developed herein were
495 inexpensive, standardizable, and practical, and can be applied by a wide range of users such as
496 aquatic researchers, commercial customers, and repository operators. Such devices would also be
497 available to other user communities (e.g., mouse researchers) that require vitrification of small
498 samples including oocytes and embryos. The utility of any type of cryopreservation device will
499 be greatly enhanced by forward thinking to include scaling options based on throughput needs,
500 and compatibility with programs for quality assurance and quality control, biosecurity, and data
501 management and integration (Liu et al., 2019; Torres and Tiersch, 2018).
502
503 **Acknowledgments**
504
505 This work was supported in part by funding from the National Institutes of Health, Office of
506 Research Infrastructure Programs (R24-OD010441 and R24-OD011120), with additional support
507 provided by the National Institute of Food and Agriculture, United States Department of
508 Agriculture (Hatch project LAB94420), the USDA NAGP-AGGRC Cooperative Agreement
509 (Award 58-3012-8-006), the Louisiana State University Research & Technology Foundation
510 (AG-2018-LIFT-003), and the LSU-ACRES (Audubon Center for Research of Endangered
511 Species) Collaborative Program. We thank W. Childress for technical assistance, T. Gutierrez-
512 Wing and N. Tiersch for discussions, and A. Lin and R, Yiu for data collection.
513

References

Animal-GRIN, 2019. Explore the Inventory of National Animal Germplasm Program. Accessed August 2019 https://nrrc.ars.usda.gov/A-GRIN/tax_inv_drilldown_page_dev?language=EN&record_source=US.

Berkovitz, A., et al., 2018. A novel solution for freezing small numbers of spermatozoa using a sperm vitrification device. Human Reproduction 33, 1975-1983.

Blackburn, H., 2011. The USDA national animal germplasm program and the aquatic species collection, in: Tiersch, T.R., Green, C. (Eds.), Cryopreservation in Aquatic Species 2nd Edition. World Aquaculture Society, Baton Rouge, LA.

Blaxter, J., 1953. Sperm storage and cross-fertilization of spring and autumn spawning herring. Nature 172, 1189.

Cuevas-Uribe, R., et al., 2017. Vitrification as an alternative approach for sperm cryopreservation in marine fishes. N. Am. J. Aquacult. 79, 187-196.

Cuevas-Uribe, R., et al., 2011a. Production of channel catfish with sperm cryopreserved by rapid non-equilibrium cooling. Cryobiology 63, 186-197.

Cuevas-Uribe, R., et al., 2011b. Production of F1 offspring with vitrified sperm from a live-bearing fish, the Green Swordtail *Xiphophorus hellerii*. Zebrafish 8, 167-179.

Cuevas-Uribe, R., et al., 2015. Vitrification of sperm from marine fish: effect on motility and membrane integrity. Aquacult. Res. 46, 1770-1784.

Devicharan, R., Garg, R., 2019. Optimization of the print quality by controlling the process parameters on 3D Printing machine, 3D Printing and Additive Manufacturing Technologies. Springer, pp. 187-194.

Fahy, G.M., Wowk, B., 2015. Principles of cryopreservation by vitrification, Cryopreservation and freeze-drying protocols. Springer, pp. 21-82.

Fernandez-Vicente, M., et al., 2016. Effect of infill parameters on tensile mechanical behavior in desktop 3D printing. 3D printing and additive manufacturing 3, 183-192.

Frauenfelder, M., 2013. Make: ultimate guide to 3D printing 2014. Maker Media, Inc.

Hagedorn, M., et al., 2019. Workshop report: Cryopreservation of aquatic biomedical models. Cryobiology 86, 120-129.

Hezavehei, M., et al., 2018. Sperm cryopreservation: A review on current molecular cryobiology and advanced approaches. Reproductive biomedicine online.

Ho, C.M.B., et al., 2015. 3D printed microfluidics for biological applications. Lab on a Chip 15, 3627-3637.

Hu, E., et al., 2017. 3-D printing provides a novel approach for standardization and reproducibility of freezing devices. Cryobiology 76, 34-40.

Hu, E., et al., 2011. High-throughput cryopreservation of spermatozoa of blue catfish (*Ictalurus furcatus*): Establishment of an approach for commercial-scale processing. Cryobiology 62, 74-82.

Huang, C., et al., 2009. Sperm cryopreservation in guppies and black mollies — a generalized freezing protocol for livebearers in Poeciliidae. Cryobiology 59, 351-356.

Jafari, R., et al., 2019. Recent progress and challenges with 3D printing of patterned hydrophobic and superhydrophobic surfaces. The International Journal of Advanced Manufacturing Technology 103, 1225-1238.

Kása, E., et al., 2017. Development of sperm vitrification protocols for freshwater fish (Eurasian perch, *Perca fluviatilis*) and marine fish (European eel, *Anguilla anguilla*). Gen. Comp. Endocrinol. 245, 102-107.

Liu, Y., et al., 2019. Development of germplasm repositories to assist conservation of endangered fishes: Examples from small-bodied livebearing fishes. Theriogenology 135, 138-151.

562 Liu, Y., et al., 2018. Production of live young with cryopreserved sperm from the endangered
563 livebearing fish Redtail Splitfin *(Xenotoca eiseni*, Rutter, 1896). Anim. Reprod. Sci. 196,
564 77-90.
565 Magnotti, C., et al., 2018. Cryopreservation and vitrification of fish semen: a review with special
566 emphasis on marine species. Reviews in Aquaculture 10, 15-25.
567 Marco-Jiménez, F., et al., 2016. Development of cheaper embryo vitrification device using the
568 minimum volume method. PLOS one 11, e0148661.
569 Polge, C., Rowson, L., 1952. Fertilizing capacity of bull spermatozoa after freezing at −79° C.
570 Nature 169, 626.
571 Purdy, P., et al., 2016. Biobanking genetic resources: challenges and implementation at the
572 USDA National Animal Germplasm Program. Reprod. Fertil. Dev. 28, 1072-1078.
573 Rall, W.F., Fahy, G.M., 1985. Ice-free cryopreservation of mouse embryos at− 196 C by
574 vitrification. Nature 313, 573-575.
575 Rayna, T., Striukova, L., 2016. From rapid prototyping to home fabrication: How 3D printing is
576 changing business model innovation. Technol. Forecast. Soc. Change 102, 214-224.
577 Riley, K.L., et al., 2004. Cryopreservation of sperm of red snapper (*Lutjanus campechanus*).
578 Aquaculture 238, 183-194.
579 Tiersch, N.J., et al., 2019. Three-dimensional printing of vitrification loop prototypes for aquatic
580 species. Zebrafish 16, 252-261.
581 Tiersch, N.J., Tiersch, T.R., 2017. Standardized assessment of thin-film vitrification for aquatic
582 species. N. Am. J. Aquacult. 79, 283-288.
583 Tiersch, T., et al., 2004. Transport and cryopreservation of sperm of the common snook,
584 Centropomus undecimalis (Bloch). Aquacult. Res. 35, 278-288.
585 Tiersch, T.R., Monroe, W.T., 2016. Three-dimensional printing with polylactic acid (PLA)
586 thermoplastic offers new opportunities for cryobiology. Cryobiology 73, 396-398.
587 Torres, L., et al., 2017. Challenges in development of sperm repositories for biomedical fishes:
588 quality control in small-bodied species. Zebrafish 14, 552-560.
589 Torres, L., Tiersch, T.R., 2018. Addressing reproducibility in cryopreservation, and
590 considerations necessary for commercialization and community development in support of
591 genetic resources of aquatic species. Journal of the World Aquaculture Society 49, 644-
592 663.
593 Wayman, W.R., et al., 2008. Cryopreservation of sperm from endangered pallid sturgeon. North
594 American Journal of Fisheries Management 28, 740-744.
595 Yang, H., et al., 2009. Sperm cryopreservation of a live-bearing fish, *Xiphophorus couchianus*:
596 male-to-male variation in post-thaw motility and production of F 1 hybrid offspring. Comp.
597 Biochem. Physiol., C: Toxicol. Pharmacol. 149, 233-239.
598 Yang, H., Tiersch, T.R., 2009. Current status of sperm cryopreservation in biomedical research
599 fish models: zebrafish, medaka, and *Xiphophorus*. Comp. Biochem. Physiol., C: Toxicol.
600 Pharmacol. 149, 224-232.
601

602

603

604 Table 1. Specifications used for 3-D printing of vitrification devices in the present study

605

Parameters	Settings
Printer name	MakerBot Replicator 2X
Slicing software	MakerBot Desktop Beta Version 3.10.1.1389
Filament material	PLA [a] and ABS [b]
Filament diameter	1.75 mm
Heat block temperature	200 °C for PLA and 230 °C for ABS
Print speed	90 mm/s for infill and 40 mm/s for outermost layers
Nozzle diameter	0.4 mm
Nominal layer height	0.2 mm
Retraction distance	1.3 mm
Retraction speed	25 mm/s
Print bed temperature	110 °C for ABS and room temperature (~25 °C for PLA)
Build surface material	ScotchBlue™ tape
Part cooling fan speed	50%
First layer printing speed	40 mm/s
Infill rate	100%
Infill pattern	Hexagonal (honey comb) pattern
Perimeter layer number	2
Top layer number	4
Bottom layer number	4
Support usage	No support applied
Build surface size	24.6 L × 15.2 W × 15.5 H cm

606

607 [a] Polylactic acid
608 [b] Acrylonitrile butadiene styrene

609

Table 2. The vitrification feasibility of samples frozen in devices fabricated with two thermoplastics (PLA and ABS), and various loop lengths, and layer numbers. Prototypes with 13 various layers and 3 lengths (10-20 mm) were evaluated. The vitrification performance was classified based on integrity and transparency of frozen film: 0 — Film failure, 1 — Opaque, 2 — Translucent, and 3 Transparent.

Layer	PLA			ABS		
number	10 mm	15 mm	20 mm	10 mm	15 mm	20 mm
1	0,3	0,0	0,0	0,3	0,3	0,0
2	3,3	0,3	0,0	3,3	0,2	0,0
3	0,3	0,3	0,0	0,2	3,3	0,0
4	2,3	0,0	0,2	2,2	0,0	0,0
5	2,3	0,0	0,2	1,2	0,0	0,0
6	1,1	2,3	0,2	1,1	0,1	0,0
7	2,2	0,0	0,2	1,2	0,2	0,0
8	1,1	0,2	0,0	1,2	0,0	0,0
9	1,2	0,1	0,0	1,1	0,1	0,0
10	1,1	1,1	0,0	1,1	0,0	0,0
11	1,1	0,0	0,0	0,2	0,0	0,0
12	1,1	0,1	0,0	1,1	0,0	0,0
13	1,1	0,0	0,0	1,1	0,0	0,0

625 **Figure Legends**

626 **Fig. 1**. Diagram of the features of a prototype 3-D printed vitrification device. Several innovative
627 elements and functions were integrated, including a loop to suspend a thin film of fluid (i.e.
628 sperm suspension), a retractable sleeve (not shown) to protect vitrified samples and allow
629 permanent labeling by ink-jet printing, a handle to facilitate processing and storage, a shaft to
630 avoid cryo-injuries to users during freezing, and annular grooves on the extension pole to guide
631 the protective retractable sleeve to the 'open' or 'closed' positions.
632
633 **Fig. 2**. Dimensional diagram of an example of prototype 3-D printed vitrification devices. The
634 loop length (LP) was 10, 15, or 20 mm, and the loop height (LH) varied between 0.2 mm and 2.6
635 mm (13 variations with 0.2-mm increments). No variations were designed for the loop width
636 (LW).
637
638 **Fig. 3**. Demonstration of the positioning of a protective retractable sleeve. The retractable sleeve
639 was placed in the "open" position during freezing and thawing, and slid to the 'closed' position
640 for storage. The retractable sleeve was adopted for prototyping purposes only from protective
641 jackets of commercially available 0.5-mL sperm cryopreservation straws (Cryo Bio System,
642 L'Aigle, France).
643
644 **Fig. 4**. Fabrication quality of a total of 97 devices fabricated with PLA filament (black bars), and
645 86 devices fabricated with ABS (grey bars). (A) Fabrication print failures of prototype
646 vitrification devices with different loop lengths and fabrication materials. (B) Actual
647 measurement of layer height increment (n = 13).
648
649 **Fig. 5**. Examples of major types of fabrication failures.
650

651 **Fig. 6**. The relationships between the sample volume capacity of water and the layer number of
652 loops for prototype vitrification devices fabricated with PLA (open circles) and ABS (closed
653 circles).
654
655 **Fig. 7**. Predicted probability of achieving vitrified (clear) samples with prototype devices
656 fabricated with ABS (solid line) and PLA (dashed line). The different loop lengths and layer
657 numbers were combined for analysis.
658

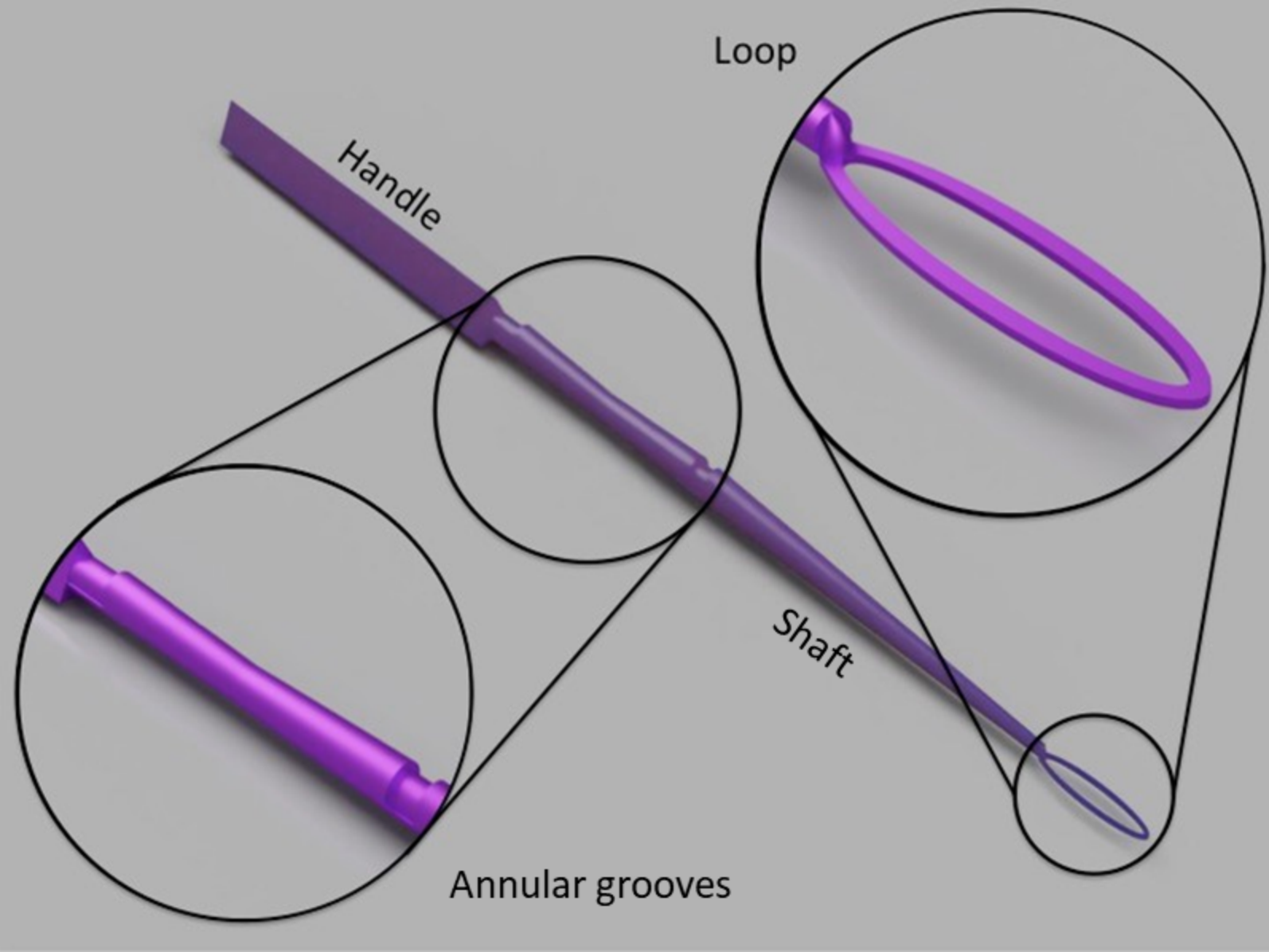
Loop
Handle
Shaft
Annular grooves

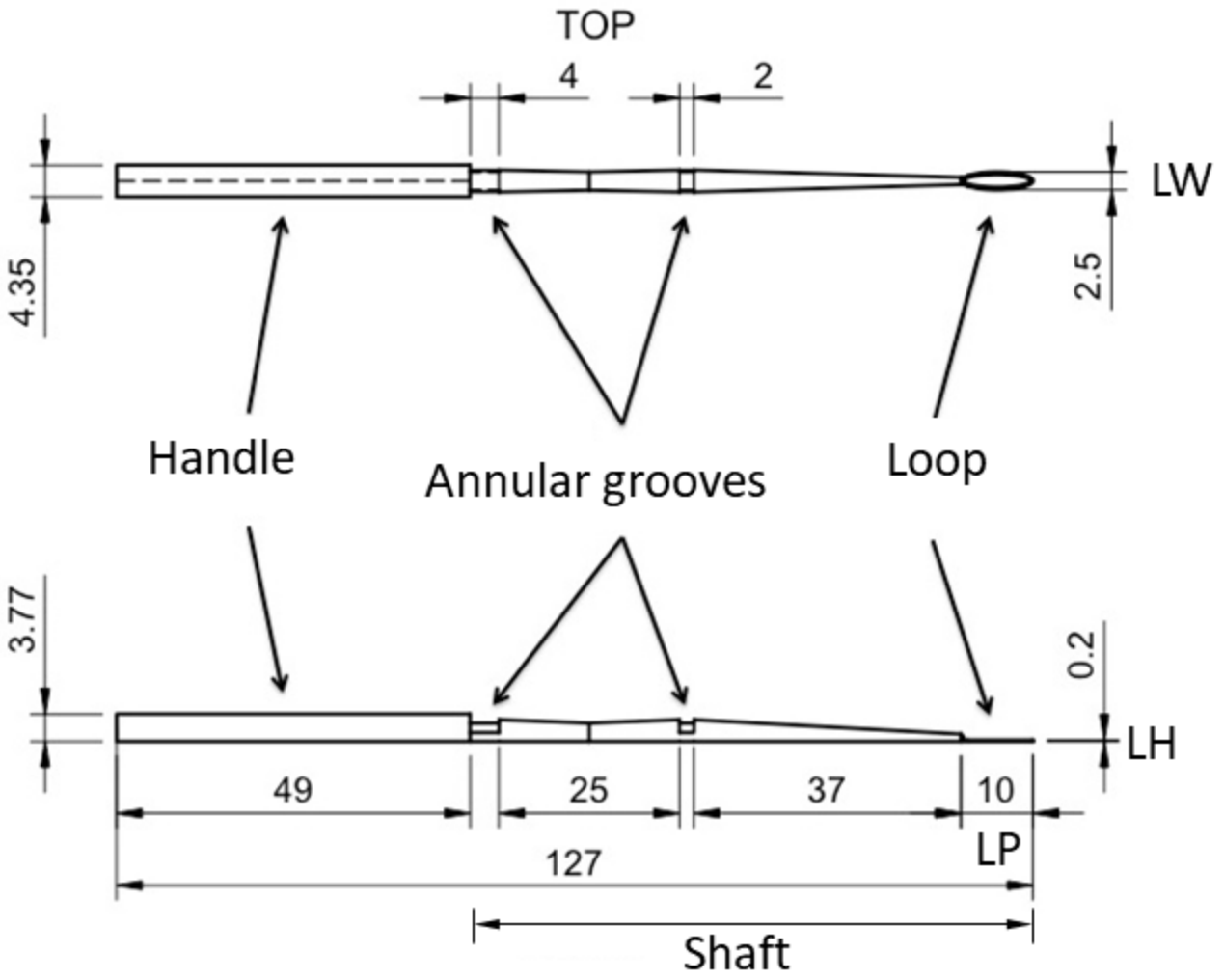

FRONT

(Dimensions in mm)

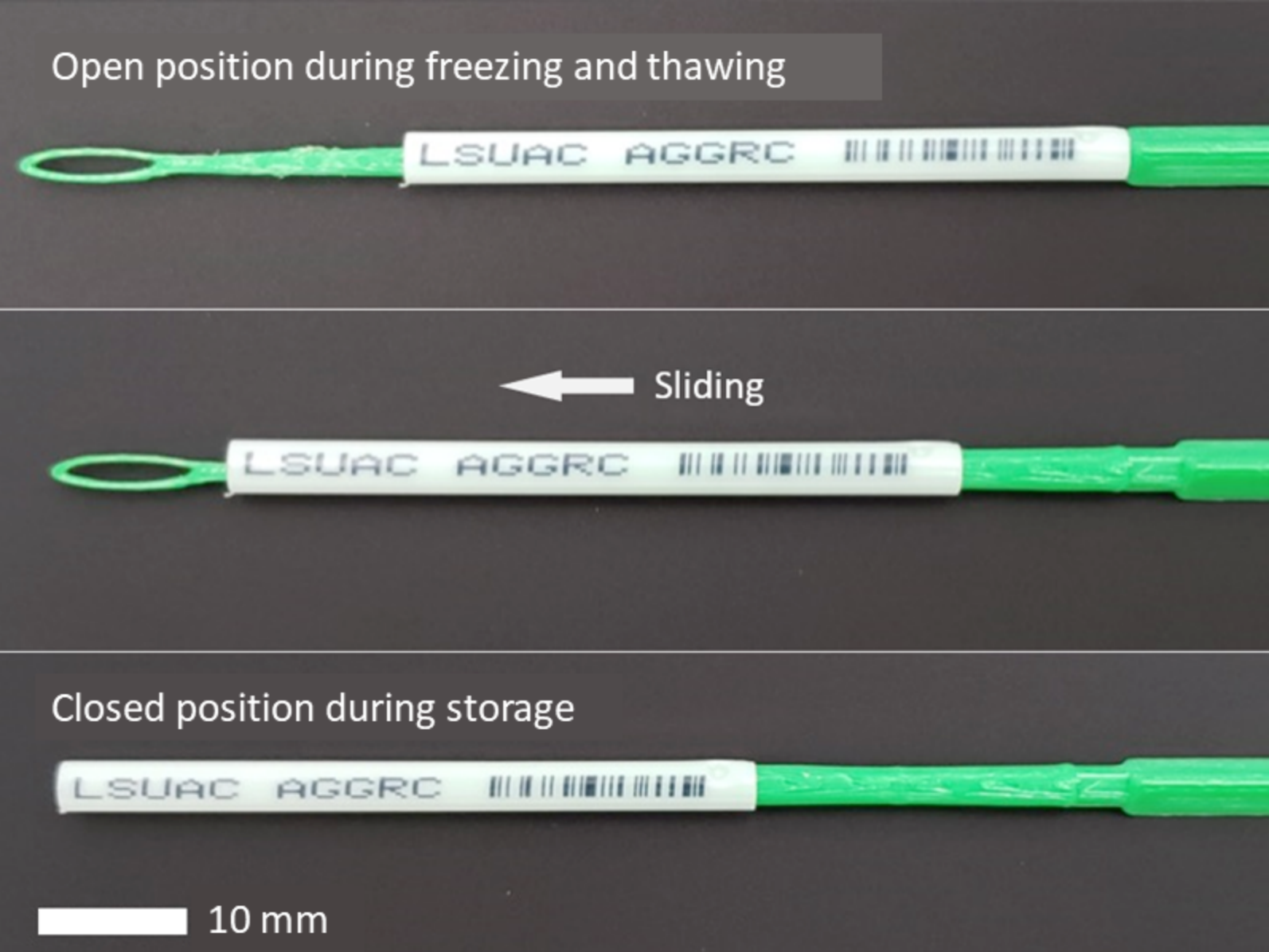
Open position during freezing and thawing
LSUAC AGGRC
Sliding
LSUAC AGGRC
Closed position during storage
LSUAC AGGRC
10 mm

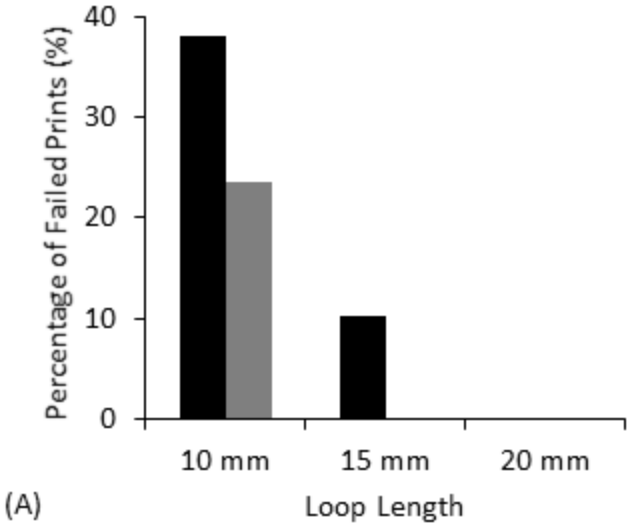
Percentage of Failed Prints (%)
40
30
20
10
0
10 mm
15 mm
20 mm
Loop Length

(A)

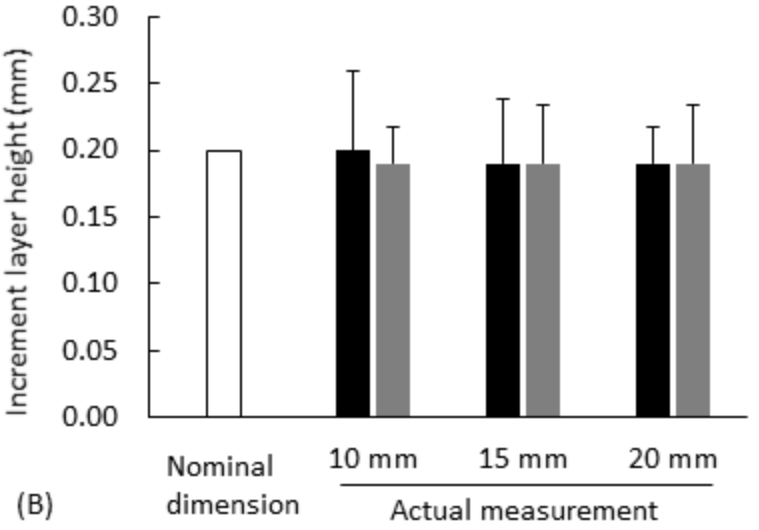
Increment layer height (mm)
0.30
0.25
0.20
0.15
0.10
0.05
0.00
Nominal dimension
10 mm
15 mm
20 mm
Actual measurement

(B)

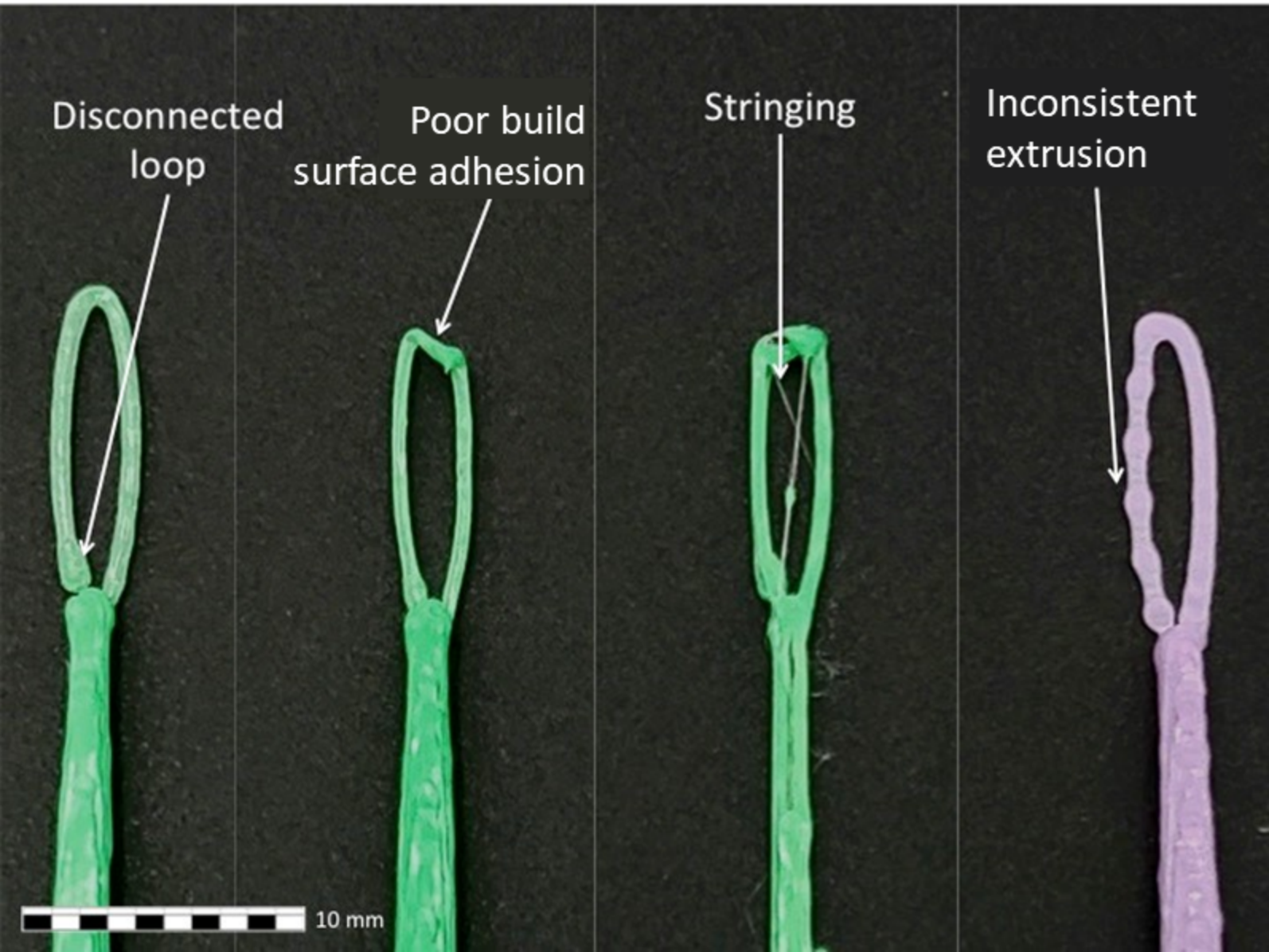
Disconnected loop
Poor build surface adhesion
Stringing
Inconsistent extrusion
10 mm

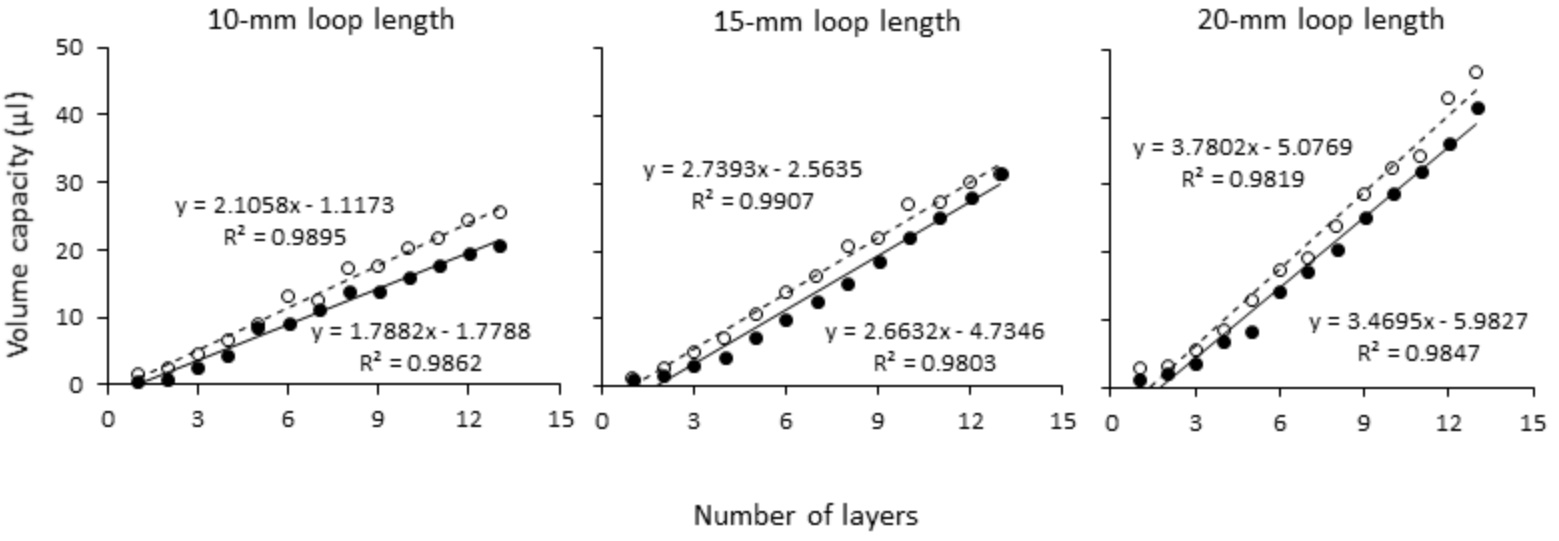
10-mm loop length
15-mm loop length
20-mm loop length
Volume capacity (µl)
Number of layers
y = 2.1058x - 1.1173
R² = 0.9895
y = 1.7882x - 1.7788
R² = 0.9862
y = 2.7393x - 2.5635
R² = 0.9907
y = 2.6632x - 4.7346
R² = 0.9803
y = 3.7802x - 5.0769
R² = 0.9819
y = 3.4695x - 5.9827
R² = 0.9847
0
10
20
30
40
50
0
3
6
9
12
15

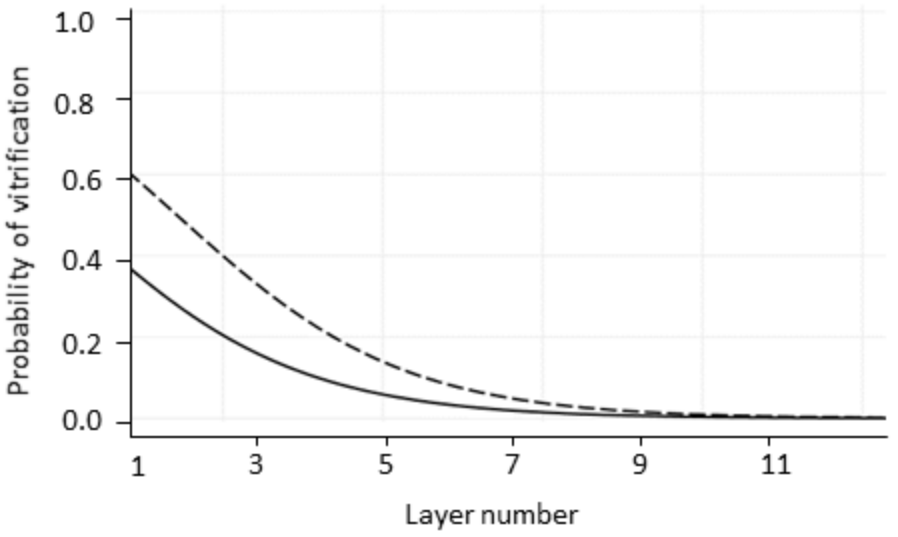
1.0
0.8
0.6
0.4
0.2
0.0
Probability of vitrification
1
3
5
7
9
11
Layer number